Green Chemistry

PAPER

View Article Online
View Journal | View Issue

Cite this: *Green Chem.*, 2021, **23**, 4170

Controlling product selectivity with nanoparticle composition in tandem chemo-biocatalytic styrene oxidation†

Derik Wilbers,[a,b] Joseph Brehm,[c] Richard J. Lewis,[c] Jacqueline van Marwijk,[d] Thomas E. Davies,[c] David J. Morgan,[c] Diederik J. Opperman,[a,d] Martha S. Smit,[a,d] Miguel Alcalde,[e] Athanasios Kotsiopoulos,[a,b] Susan T. L. Harrison,*[a,b] Graham J. Hutchings*[c] and Simon J. Freakley*[f]

The combination of heterogeneous catalysis and biocatalysis into one-pot reaction cascades is a potential approach to integrate enzymatic transformations into existing chemical infrastructure. Peroxygenases, which can achieve clean C–H activation, are ideal candidates for incorporation into such tandem systems, however a constant supply of low-level hydrogen peroxide (H_2O_2) is required. The use of such enzymes at industrial scale will likely necessitate the *in situ* generation of the oxidant from cheap and widely available reactants. We show that combing heterogeneous catalysts (Au_xPd_y/TiO_2) to produce H_2O_2 *in situ* from H_2 and air, in the presence of an evolved unspecific peroxygenase from *Agrocybe aegerita* (PaDa-I variant) yields a highly active cascade process capable of oxidizing alkyl and alkenyl substrates. In addition, the tandem process operates under mild reaction conditions and utilizes water as the only solvent. When alkenes such as styrene are subjected to this tandem oxidation process, divergent reaction pathways are observed due to the competing hydrogenation of the alkene by palladium rich nanoparticles in the presence of H_2. Each pathway presents opportunities for value added products. Product selectivity was highly sensitive to the rate of reduction compared to hydrogen peroxide delivery. Here we show that some control over product selectivity may be exerted by careful selection of nanoparticle composition.

Received 22nd December 2020,
Accepted 7th May 2021

DOI: 10.1039/d0gc04320f

rsc.li/greenchem

Introduction

The activation of hydrocarbons while preventing deep oxidation to CO_2 remains a challenge in heterogeneous catalysis. The development of new processes to install oxygen functionality selectively into C–H bonds while operating under energy efficient and green process conditions is of significant economic importance.[1–4] Oxygenates produced by such processes may be sold as value-added products or as platform chemicals in diverse supply chains that include the pharmaceutical or fine chemical industries.[1] Traditional chemocatalytic hydrocarbon oxidation routes are often inefficient due to operation under harsh reaction conditions, limited product selectivity and the use of environmentally unfriendly oxidants, particularly at lab scale, such as *tert*-butyl hydroperoxide (TBHP),[5] benzoylperoxide and *meta*-chloroperoxybenzoic acid (*m*CPBA).[6,7] Enzymatic processes are a highly attractive approach for use in hydrocarbon oxidation reactions due to the typically high stereo- and chemoselectivity of certain classes of biocatalysts. A number of heme-containing enzymes such as the cytochrome P450 family are highly active and selective biocatalysts for substrate specific C–H activations and epoxidations, but their dependency on sacrificial redox cofactors and auxiliary flavoproteins when using O_2 can increase both the complexity as well as the cost of a potential oxidative process.[8–12] Unspecific peroxygenases (UPOs) are extracellular heme-thiolate enzymes of fungal origins, capable of various 1 and 2-electron oxidative transformations on a wide range of substrates.[13,14] UPOs can utilize H_2O_2 as both electron accep-

[a]*South African DST-NRF Centre of Excellence in Catalysis, C*Change, University of Cape Town, Private Bag, Rondebosch, 7701, Cape Town, South Africa. E-mail: Sue.Harrison@uct.ac.za*
[b]*Centre for Bioprocess Engineering Research (CeBER), Department of Chemical Engineering, University of Cape Town, Private Bag X3, Rondebosch, 7701, Cape Town, South Africa*
[c]*Cardiff Catalysis Institute, School of Chemistry, Cardiff University, Main Building, Park Place, Cardiff, CF10 3AT, UK. E-mail: Hutch@Cardiff.ac.uk*
[d]*Department of Microbial, Biochemical and Food Biotechnology, University of the Free State, Bloemfontein, South Africa*
[e]*Institute of Catalysis, ICP-CSIC, Cantoblanco, 28049 Madrid, Spain*
[f]*Department of Chemistry, University of Bath, Claverton Down, Bath, BA2 7AY, UK. E-mail: s.freakley@bath.ac.uk*

†Electronic supplementary information (ESI) available. See DOI: 10.1039/d0gc04320f

tor and oxygen donor to functionalize C–H bonds without the need of a complex electron transport chain or co-factors that need to be regenerated.[15] Due to this benefit, UPOs have been identified as potential industrial biocatalysts for a variety of oxidative transformations.[16]

UPOs are however highly sensitive towards H_2O_2 concentration. A large excess of H_2O_2 can result in oxidative damage to the enzyme itself, leading to a loss of activity. In order to circumvent this deactivation, a number of H_2O_2 delivery methods to UPOs have been reported. These include the use of enzyme cascades (glucose oxidase/peroxygenase[17,18] and formate oxidase/peroxygenase systems[19,20]) oxidase and peroxygenase fusions,[21] and a number of heterogeneous chemo- and photocatalysts.[22–25] Among heterogenous catalysts, Au_xPd_y bimetallic nanoparticles on various supports have been reported as highly active catalysts for H_2O_2 direct synthesis.[23,26,27] We reasoned that such Au_xPd_y bimetallic nanoparticles might find further utility in a chemo-bio tandem system when employing peroxygenases to upgrade alkenes.

We recently reported on such a tandem catalytic system composed of metal nanoparticles and the laboratory-evolved UPO from *Agrocybe aegerita* (PaDa-I variant) for selective oxidation of C–H bonds.[22] In this work, we designed a one-pot system in which metal nanoparticles catalyzed the *in situ* formation of H_2O_2 from a H_2/air mixture at a rate and concentration appropriate for subsequent enzymatic peroxygenase activity. This combination could remove the need to transport, store and dilute concentrated H_2O_2 solutions on translation to a large scale. One-pot reaction setups can be attractive from an industrial point of view due to fewer expensive separation and purification steps typically being required. However, process conditions are often confined to narrow operating windows to ensure compatibility between the different catalytic processes. In this case, we were able to operate the catalytic system in one-pot, at ambient temperature and relatively low pressures while employing buffered aqueous solutions as the solvent. Under these reaction conditions a range of different alkane substrates including cyclohexane and ethylbenzene were successfully oxidized to various oxygen-containing products with high chemo selectivity, retaining the advantage of high enantiomeric excess associated with biocatalytic transformations and achieving some of the highest turnover numbers yet reported.[22]

When employing alkenes as reaction substrate in our one-pot system, the reduction of the alkenyl moiety by the Pd containing catalysts in the presence of H_2 becomes a competing reaction and much more complex product distributions are observed. This requires a greater understanding of the reaction networks as the heterogeneous catalyst not only dictates the amount of H_2O_2 produced but also catalyzes primary reactions with the substrate that compete with enzymatic oxidation. In this manner a greater number of potential products could be obtained by cascading bio and heterogeneous catalytic reactions and process selectivity may thus be controlled by variation of chemocatalyst composition. In this paper we aim to demonstrate that control of the reaction cascade, in terms of the order of enzymatic and heterogeneous catalytic steps can result in the production of primary or secondary alcohols from a terminal alkene substrate.

Results and discussion

Styrene was selected as model alkene substrate as it has an activated double bond due to the presence of an aromatic ring while possessing no allylic carbons as sites for direct hydroxylation by the PaDa-I enzyme. Industrially the production of styrene oxide from styrene is commonly carried out by either chlorohydrin-based routes involving sequential chlorination–dehydrochlorination cycles or reactions involving benzoyl peroxide.[28–30] These reactions are undesirable from a green chemistry point of view as the chlorination–dechlorination route produces a large amount of hazardous waste. Attempts to facilitate oxidation at milder conditions using radical initiators such as TBHP and H_2O_2 are typically carried out at elevated temperature and can often result in the isomerisation of styrene oxide to benzaldehyde. Styrene oxide, resulting from the epoxidation of styrene, is an important industrial chemical while 2-phenylethanol resulting from ring opening of the styrene oxide finds application in the fragrance, cosmetics and food industry.[31] These are both potential products of the reaction cascade if the styrene undergoes an epoxidation reaction catalyzed by PaDa-I using the *in situ* produced H_2O_2 followed by hydrogenative ring opening in the presence of the heterogeneous metal catalyst and gas phase H_2 (Scheme 1, Pathway 1). The demonstration of a possible one pot route to the fragrance molecule 2-phenylethanol from styrene has potential to replace sequential oxidative and reductive reactions which require multiple stage catalytic processes. Alternatively, the styrene may be reduced by the Pd rich catalysts in the presence of H_2 to form ethylbenzene. The formed ethylbenzene can then undergo C–H activation, catalyzed by PaDa-I using H_2O_2 as oxidant, to form 1-phenylethanol. PaDa-I selectively produces the secondary alcohol from ethylbenzene hydroxylation (Scheme 1, Pathway 2) in high enantiomeric excess.[22] By controlling the reaction rates of the first catalytic transformation of styrene, it is in principle possible to produce either the primary or secondary alcohol from the terminal alkene reactant. The realization of a tandem hetero-bio reaction system would lead to the demonstration of a route to process intensification removing the need to produce and store concentrated H_2O_2 solutions. In contrast to current industrial technologies (described above), the activation of C–H and C=C bonds at mild conditions (aqueous solutions, ambient temperatures, near ambient pressure) and producing only water as a by-product is an attractive green technology.

Our initial studies established the efficacy of a series of 1% Au_xPd_y/TiO_2 catalysts, of varying Au : Pd ratio, towards the direct synthesis and subsequent degradation of H_2O_2 under conditions previously optimized for H_2O_2 formation (Table S1†). Consistent with previous studies,[32] we observe that an enhancement in catalytic performance can be achieved through the combination of Au and Pd, with H_2O_2 synthesis

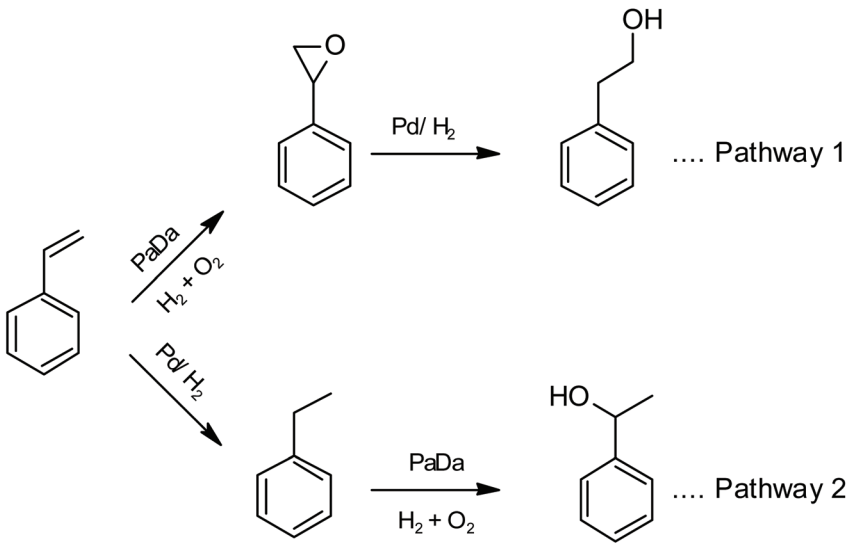

Scheme 1 Divergent reaction pathways observed for the tandem oxidation of styrene.

rates of the $Au_{50}Pd_{50}/TiO_2$ catalyst (94 $mol_{H_2O_2}$ kg_{cat}^{-1} h^{-1}) far greater than that observed with the corresponding monometallic analogues when tested at elevated pressures. Measurement of the mean nanoparticle size of the various catalysts (Table 1) as determined by bright field transmission electron microscopy (BF-TEM) (Fig. S1†) reveals that the $Au_{50}Pd_{50}/TiO_2$ catalyst displays the smallest mean particle size (4.2 ± 1.8 nm) amongst the catalysts with a comparatively narrow size distribution. In contrast the other bimetallic nanoparticles have much wider size distributions and, in some cases, large particles around 40 nm are observed. Similar nanoparticle size distributions have been previously reported by us for analogous systems with detailed studies indicating that such large particles are typically very rich in Au with little to no alloying to Pd and as a result are much less active for H_2O_2 synthesis.[32,33] Further analysis of the as-prepared Au_xPd_y catalysts *via* X-ray photoelectron spectroscopy (Fig. S2 and Table S2†) indicates that the introduction of Au into a monometallic Pd catalyst significantly modifies Pd-oxidation state, with a shift towards Pd^{2+} upon Au incorporation. The presence of domains of mixed Pd oxidation state has been well reported to improve catalytic performance towards H_2O_2 synthesis.[34,35]

Table 1 Mean particle size of 1% Au_xPd_y/TiO_2 catalysts, prepared *via* an excess chloride impregnation methodology, as determined by transmission electron microscopy

Catalyst	Mean particle size/nm (standard deviation)
Au_{100}/TiO_2	24.9 (7.9)
$Au_{75}Pd_{25}/TiO_2$	13.1 (8.3)
$Au_{50}Pd_{50}/TiO_2$	4.2 (1.8)
$Au_{25}Pd_{75}/TiO_2$	6.5 (8.5)
Pd_{100}/TiO_2	n.d.[a]

[a] Unable to determine due to particle sizes being below TEM limits of detection.

Both H_2 and O_2 are known to easily dissociate over Pd^0 sites, whereas O_2 is stable over PdO surfaces.[36–38] As such the presence of Pd–PdO domains is likely a key factor responsible for the enhanced activity observed for the optimal $Au_{50}Pd_{50}/TiO_2$, promoting the dissociation of adsorbed H_2, while preventing the cleavage of the O–O bond, which would result in the unselective production of water.

Building on these studies we next evaluated the performance of the supported 1% Au_xPd_y/TiO_2 catalysts towards H_2O_2 synthesis, under conditions identical to those that had been previously utilized for the UPO with the addition of gaseous reactants (2 bar, 80% H_2, 20% air) (Fig. 1). The results demonstrate that even at conditions that are significantly milder than those optimized for H_2O_2 synthesis (high pressure, alcohol/water solvent systems, high agitation) it is possible to produce H_2O_2 concentrations of 5–20 ppm with all catalyst systems that contain Pd. The Au_{100}/TiO_2 catalyst did not produce measurable concentrations of H_2O_2 during the test. The Pd_{100}/TiO_2 had the highest initial rate for H_2O_2 synthesis; however, over time the concentration of H_2O_2 in solution decreased due to the higher rates of subsequent H_2O_2 degradation that occur on monometallic Pd catalysts. In contrast, the $Au_{50}Pd_{50}/TiO_2$ catalyst showed comparable high initial rates and was able to sustain a consistent concentration of H_2O_2 (15 ppm) throughout the test due to a reduced rate of H_2O_2 degradation which has been reported for this class of catalyst.[32] This H_2O_2 concentration is near optimal for sustained operation of the UPO PaDa-I according to previous studies.[16,39]

We next evaluated the performance of the supported Au_xPd_y/TiO_2 catalysts when used in tandem with PaDa-I, for the oxidation of styrene (Table 2) in a one-pot system. The Au_{100}/TiO_2 catalyst exhibited very low levels of product formation in the tandem system, within the errors of our analysis, which is unsurprising given the limited activity of monometallic Au catalysts towards both the direct synthesis of H_2O_2 and

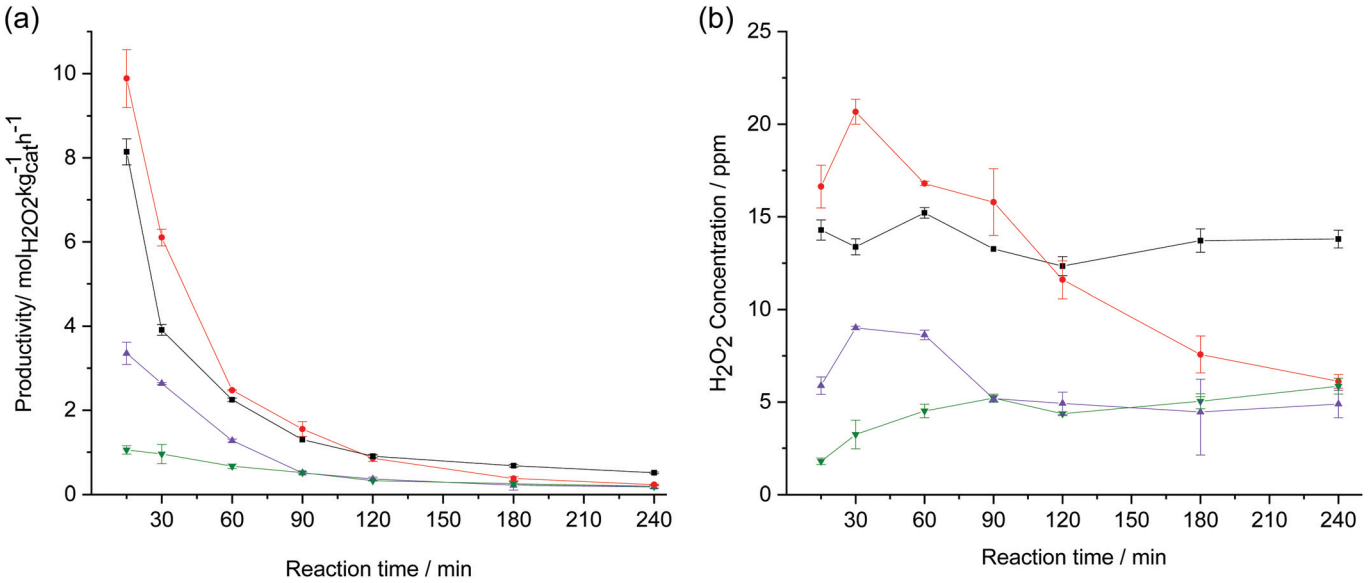

Fig. 1 (a) Net H_2O_2 productivity by various Au–Pd nanoparticles as a function of Au : Pd (b) concentration of H_2O_2 observed in solution as a function of Au : Pd. Key: $Au_{25}Pd_{75}/TiO_2$ (purple triangles), $Au_{50}Pd_{50}/TiO_2$ (black squares), $Au_{75}Pd_{25}/TiO_2$ (green inverted triangles), Pd_{100}/TiO_2 (red circles). H_2O_2 direct synthesis reaction conditions: Catalyst (2 mg), phosphate buffer (10 mL, pH 6.0), using a gas mixture of 80% H_2/Air (1.6 bar H_2, 0.4 bar air, 2 bar), 200 rpm.

Table 2 Obtained product selectivities and activity for the tandem oxidation/reduction of styrene employing various Au–Pd nanoparticles supported on TiO_2

	Product selectivity (%)					
	Pathway 1		Pathway 2			
Catalyst	Styrene oxide	2-Phenylethanol	Ethylbenzene	1-Phenylethanol	Styrene conversion (%)	Total turnover number[a] ($\times 10^3$)
Au_{100}/TiO_2	0	0	100	0	<1	0[b]
$Au_{75}Pd_{25}/TiO_2$	27	2	68	3	39	6.8
$Au_{50}Pd_{50}/TiO_2$	40	0	58	2	37	8.6
$Au_{25}Pd_{75}/TiO_2$	7	4	82	6	66	6.7
Pd_{100}/TiO_2	6	1	92	1	48	2.0

Reaction conditions: Substrate concentration – 20 mM, heterogeneous catalyst (2 mg), PaDa-I (15 U mL^{-1}), phosphate buffer (10 mL, pH 6.0), stirred (200 rpm) for 1 hour at 25 °C, 2 bar (80% H_2, 20% air). [a] Total enzymatic turnovers to oxidised products. [b] No oxidation products detected.

alkene hydrogenation, under these reaction conditions.[40,41] By comparison, use of the Pd-only catalyst resulted in far greater activity (48% styrene conversion), with high selectivity (92%) towards ethylbenzene, again this may be expected given that Pd is known to be a highly active hydrogenation catalyst.

These observations alone may lead to the conclusion that increasing Pd content would typically favor the fast hydrogenation of styrene followed by hydroxylation of the alkyl C–H bond (Pathway 2 as shown in Scheme 1). A set of experiments was performed in the absence of the enzyme in order to test the catalytic styrene hydrogenation activity of the Au_xPd_y/TiO_2 catalysts. All ratios of Au_xPd_y/TiO_2 (apart from Au_{100}/TiO_2) exhibited quantitative conversion of the styrene to ethylbenzene within 1 hour, under our standard reaction conditions and 1.6 bar of H_2. Despite this, catalysts containing AuPd bimetallic nanoparticles were able to also produce significant amounts of oxygenated products derived from the epoxidation of styrene by the PaDa-I. In particular the $Au_{50}Pd_{50}/TiO_2$ sample which produced the highest consistent H_2O_2 concentrations could obtain 40% styrene oxide selectivity under these reaction conditions. This suggests that if the nanoparticles can also effectively catalyze the direct H_2O_2 synthesis, the driving force behind Pathway 1, the balance between the rates of H_2O_2 synthesis and styrene hydrogenation will dictate the observed reaction selectivity and this is dependent on the heterogeneous catalyst composition. A comparison of the relative selectivity to Pathway 1 and 2 combined with H_2O_2 synthesis activity as a function of heterogeneous catalyst composition is shown in Fig. 2.

Considering the two extremes in selectivity for each pathway, the Pd_{100}/TiO_2 catalyst rapidly produced H_2O_2 in the initial stages of the reaction after which a drop in H_2O_2 con-

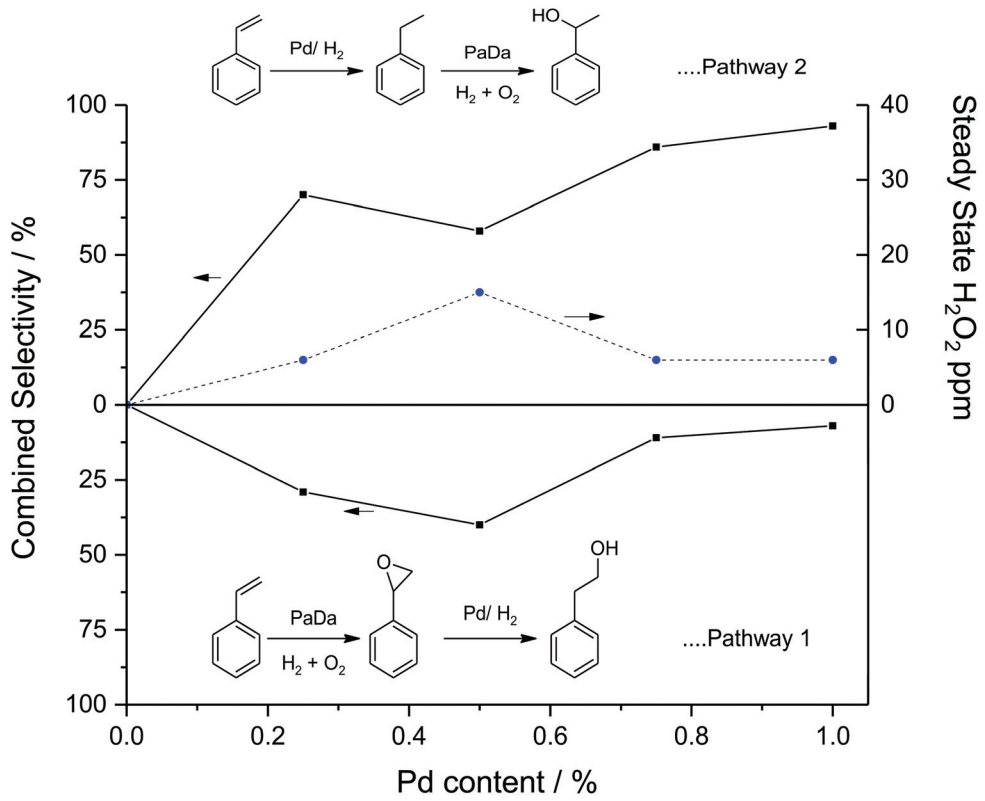

Fig. 2 Pathway selectivity with increasing Pd content from Table 2 (left axis) superimposed on steady state H_2O_2 concentration determined from 4 h tests in Fig. 1b (right axis). Combined pathway selectivity calculated as ∑(styrene oxide, 2-phenylethanol) and ∑(ethylbenzene, 1-phenylethanol) as a percentage of total reaction products. Conversion values can be found in Table 2.

centration is observed (Fig. 1b). However, only low concentrations of Pathway 1 products were observed in our tandem test reactions. Although H_2O_2 is rapidly produced in the early stages of the reaction, the Pd_{100}/TiO_2 catalyst is likely the most active catalyst for styrene hydrogenation and degradation of the formed H_2O_2. This coupled with the high rate of C=C hydrogenation relative to the enzymatic oxidation reaction, can explain the observed preference for Pathway 2 over Pathway 1 in this system. The $Au_{50}Pd_{50}/TiO_2$ catalyst on the other hand exhibited similarly high activity for H_2O_2 production but also produced products derived from a primary interaction of the substrate with the enzyme in high selectivity (40%). The decreased amounts of Pd in this catalyst, resulting in lower styrene hydrogenation activity relative to the Pd_{100}/TiO_2 catalyst with similarly high reactivity in the synthesis of H_2O_2 likely explains the high Pathway 1 selectivity achieved. Alternatively, the PaDa-I enzyme might be inhibited by the high H_2O_2 concentrations in the initial stages of the reaction when using the Pd_{100}/TiO_2 (shown in Fig. 1b). This would cause the styrene hydrogenation reaction to dominate and low selectivity for products along Pathway 1 (Table 2). The above hypothesis was evaluated by monitoring residual enzyme activity with increasing reaction time under our conditions. It was found that enzyme deactivation occurs rapidly during the initial stages of the reaction with residual enzyme activity of 56% observed after only 20 min of reaction. After this, subsequent enzyme deactivation appears to be reduced with 50% and 21% residual enzyme activities observed after 1 and 24 h respectively. This initial enzyme deactivation is likely taking place due to the sudden increase in the concentration of organic substrate and H_2O_2 at the start of the reaction.

Based on the high selectivity towards Pathway 1 products, the $Au_{50}Pd_{50}/TiO_2$ catalyst was selected for further experimentation. A study to determine the product distribution with respect to time online was then performed (Fig. 3 – split into (i) primary reaction products (ii) ethylbenzene derived products (iii) styrene oxide derived products).

A maximum of styrene oxide yield (Pathway 1) is achieved after 1 hour of reaction time. The formed styrene oxide is then converted to 2-phenylethanol by hydrogenative ring opening between 1 and 4 hours. After 2 hours of reaction the starting material has been mostly consumed by a combination of epoxidation and hydrogenation reactions and no further styrene oxide can form. The hydrogenation reaction is dominant during the early stages of the reaction and a high concentration of ethylbenzene is produced even at relatively short reaction times. The formed ethylbenzene is then converted to 1-phenylethanol, the major reaction product at long reaction times, *via* enzymatic oxidation by the PaDa-I/H_2O_2 system which we have previously shown to retain the high ee (98%)

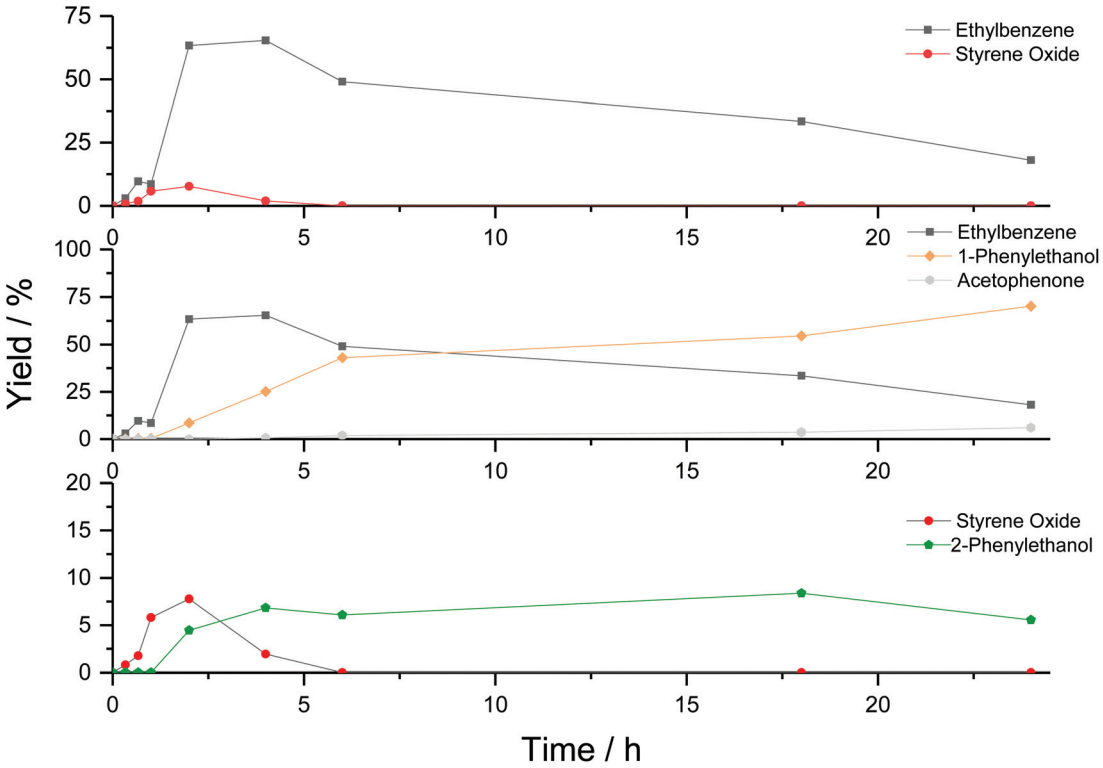

Fig. 3 Reaction yield as a function of time obtained for a $Au_{50}Pd_{50}/TiO_2$ catalyzed reaction. Reaction conditions: Substrate concentration – 20 mM, heterogeneous catalyst (2 mg), PaDa-I (15 U mL^{-1}), phosphate buffer (10 mL, pH 6.0), stirred (200 rpm) at 25 °C, 2 bar (80% H_2, 20% air).

associated with enzymatic hydroxylation of ethyl benzene derived from styrene hydrogenation.[22] The over-oxidation of 1-phenylethanol to acetophenone is also observed at extended reaction times, in excess of 15 h. At the end of the reaction the total enzymatic turnover number was 39 700.

The tandem catalytic system proved to be highly active in the transformation of styrene. However, if styrene is replaced by α-methylstyrene as substrate, a sharp decrease in catalytic activity is observed. Under the same reaction conditions (employing the $Au_{50}Pd_{50}/TiO_2$ as heterogeneous catalyst) as reported above for styrene, only traces of oxygenated products and the reduced compound, cumene, were observed after 1 hour of reaction. Increasing the reaction time to 4 hours yielded a substrate conversion of 28%. Under these conditions 2-phenyl-propane-1,2-diol (determined by GC-MS), likely formed by hydrolysis of the epoxide, was the major product of the reaction (78%) while other Pathway 1 (epoxidation first) products were observed in a combined selectivity of 5%. The heterogenous catalyst ($Au_{50}Pd_{50}TiO_2$) was much less active for the reduction of α-methylstyrene than styrene, with cumene forming in relatively low selectivity (18%). After 24 h, near quantitative conversion of α-methylstyrene is achieved. High selectivity towards products along Pathway 1 is maintained (81% combined selectivity). At such extended reaction times, 2-phenylpropan-2-ol (6%), formed by the enzymatic oxidation of cumene (13%) is also observed. Previous studies have shown that PaDa-I is highly selective towards secondary carbons during C–H activation reactions.[22] Cumene does not possess a seconday carbon for activation, thus the lower activity for the production of 2-phenylpropan-2-ol is to be expected.

In an attempt to circumvent the fast reduction of styrene and therefore obtain a clearer picture of enzyme specificity, an alternative method of *in situ* H_2O_2 generation was investigated. The metal catalyst was replaced with glucose oxidase (GOX) and glucose as a H_2O_2 delivery system. A competition experiment was then performed by generating H_2O_2 *in situ* with GOX (removing the Pd catalyzed hydrogenation of styrene) while in the presence of styrene and ethylbenzene in equimolar amounts to determine the enzyme preference for styrene epoxidation *vs.* C–H hydroxylation of ethylbenzene, (10 mM of each component was used for comparison to standard substrate loading of 20 mM styrene only). Under these metal free conditions PaDa-I preferentially epoxidized styrene to styrene oxide (78% selectivity), with comparatively much less oxidation of the ethyl benzene to 1-phenylethanol (22% selectivity) observed. Relative to the GOX/PaDa-I system, the Au_xPd_y/TiO_2 catalysts (with exception of the $Au_{50}Pd_{50}/TiO_2$) exhibited poor selectivity towards products along Pathway 1, due to the high catalytic activity exhibited for the styrene hydrogenation reaction.

Based on this observation and in a further attempt to suppress alkene hydrogenation in this system, the use of Lindlar's catalyst (Alfa Aesar) was investigated as a means to inhibit the

alkene hydrogenation reaction, which initiates reaction Pathway 2. Lindlar's catalyst is reported to selectively reduce alkynes to alkenes but not alkenes to alkanes.[42] Lindlar's catalyst consists of Pd nanoparticles (typically large and poorly defined) supported on $CaCO_3$ and poisoned with lead.[43] To the best of our knowledge this catalyst has never been tested for H_2O_2 synthesis; however, we show that under our optimized conditions (Table S1†) the catalyst has very high levels of H_2O_2 degradation activity. Under our standard H_2O_2 synthesis conditions, the Lindlar catalyst performed poorly compared to the Au_xPd_y/TiO_2 catalysts, however, small amounts of H_2O_2 were formed under our tandem reaction test conditions. Initial results of the Lindlar/PaDa-I tandem system (Table 3, entry 1) were promising with the Lindlar catalyst achieving relatively high selectivity towards styrene oxide although at very low substrate conversion. This selectivity was maintained for up to four hours, however, at longer reaction times (24 h) the selectivity towards Pathway 1 products is lost.

This could be an indication that the Lindlar catalyst is deactivating the enzyme over the course of the reaction, with very little enzyme activity left after 24 hours. This would also explain the low 1-phenylethanol selectivity observed after 24 hours even though a high concentration of ethylbenzene is formed. The deactivation of various different enzymes by heavy metals in solution have previously been reported.[44–46] Lead, present in small quantities within the Lindlar catalyst is known to bind to disulfide bonds and cysteine residues potentially precipitating and deactivating enzymes.[47] Such moieties are also present in PaDa-I, but to the best of our knowledge such deactivation studies have not yet been performed on PaDa-I.[39,48] It was hoped that by employing the Lindlar catalyst no alkene reduction would be observed. Unfortunately, the double bond in styrene is likely too active and reduction of this moiety is observed, particularly at longer reaction times.

While the Lindlar catalyst/PaDa-I system exhibited high selectivity towards styrene oxide at short reaction times, no 2-phenylethanol, expected to form during the ring opening of styrene oxide, was detected. This observation lead us to further study the catalytic ring opening of styrene oxide using the Au_xPd_y systems. Sasu *et al.* reported on supported Co and Ni catalysts for the hydrogenation of styrene oxide to 2-phenylethanol in a cascade process.[49] Other authors have investigated the production of 2-phenylethanol from styrene oxide. Under their process conditions deoxygenation and reduction to ethylbenzene was also observed and lead to the formation of styrene and ethylbenzene as side products. Various supported palladium catalysts have also been reported for this process, some of which are highly selective towards the formation of 2-phenylethanol.[50,51]

Under our reaction conditions, the Lindlar catalyst was relatively inactive for the hydrogenation of styrene oxide, as might be expected from the low 2-phenylethanol selectivities reported in Table 3 (short reaction times). In contrast, Au_xPd_y/TiO_2 catalysts were much more active, with the $Au_{50}Pd_{50}/TiO_2$ catalyst converting more than 60% of the starting material after 1 h (Fig. 4). This observation demonstrates that if the initial reaction selectivity can be steered towards the production of styrene oxide using Au_xPd_y catalysts, high yields of 2-phenylethanol can be achieved. Under our reaction conditions using the Au_xPd_y/TiO_2 catalysts, 2-phenylethanol was produced selectively with no other products detected *via* GC analysis.

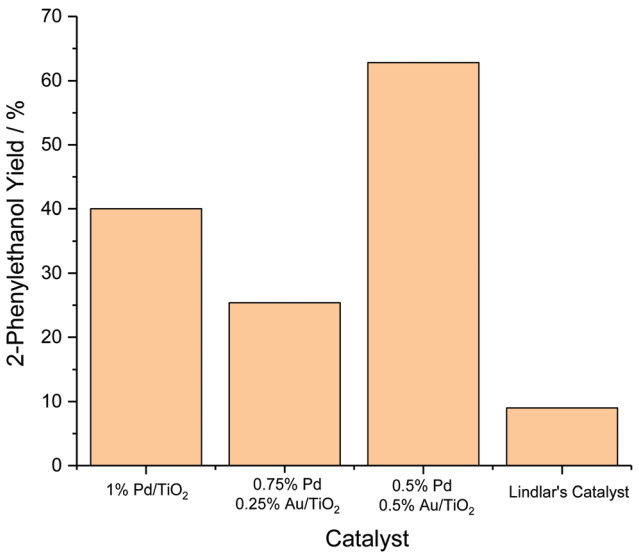

Fig. 4 Hydrogenation of styrene oxide to 2-phenylethanol. Reaction conditions: Substrate concentration – 20 mM, heterogeneous catalyst (2 mg containing 1wt% metal, apart from Lindlar's catalyst (5wt%)). 20 mM styrene oxide, phosphate buffer (10 mL, pH 6.0) and stirred for 1 hour at 25 °C, 2 bar (80% H_2, 20% air).

Table 3 The application of Lindlar's catalyst in the tandem oxidation of styrene

	Product selectivity (%)/(yield%)				
	Pathway 1		Pathway 2		
Time (h)	Styrene oxide	2-Phenylethanol	Ethylbenzene	1-Phenylethanol	Styrene conversion (%)
1	45 (2)	0 (0)	55 (2)	0 (0)	4
4	46 (10)	0 (0)	54 (11)	0 (0)	21
24	0 (0)	7 (7)	83 (83)	10 (10)	100

Reaction conditions: Substrate concentration 20 mM, heterogeneous catalyst (2 mg), PaDa-I (15 U ml^{-1}), phosphate buffer (10 mL, pH 6.0), stirred for 1 h at 25 °C, 2 bar (80% H_2, 20% air).

The stability of the PaDa-I enzyme in tandem systems is of paramount importance. Production and purification of the enzyme is a time-consuming and expensive process. The feasibility of this tandem process depends on the ability to recycle the chemo- and biocatalysts. The TiO_2 supported nanoparticle catalysts have been shown to be recyclable up to three times without significant loss in activity.[33] Our previous studies using this system for ethylbenzene hydroxylation (Pathway 2) have demonstrated that much higher substrate concentrations can potentially be tolerated compared to the 20 mM used for the screening reactions in this study. We have previously reported that on addition of 90 mM of substrate over 64 h (3 × 30 mM addition with gas recharging) the tandem system was able to produce 46 mM of 1-phenylethanol and 14 mM of acetophenone.[22] This represented a total enzymatic turnover number of 201 000 with possible accumulation of reaction products limiting activity. To extend the lifetime of these tandem systems further, future studies will explore the effects of product inhibition in more complex reaction systems and the possibility of continuous product extraction or continuous flow processes using immobilized enzymes. Apart from enzyme lifetime and catalyst recyclability, analysis of byproducts and the associated cost of their disposal can have a huge impact on process feasibility.

In contrast to the previously described chlorination–dehydrochlorination process,[28–30] enzymatic oxidation employing H_2O_2 can occur with higher relative atom economy (AE) as water is the only side product formed. Previous studies by Notari have directly compared the atom economies for the closely related oxidation of propene to propene oxide *via* the chlorohydrin and H_2O_2 based epoxidation processes.[52,53] Due to the large amounts of inorganic halide salts formed by the traditional chlorohydrin route, the atom economy is low (25%) while the catalyzed hydrogen peroxide oxidation was considerably higher atom economy of 76%. A similar trend is observed for the oxidation of styrene to styrene oxide which occurs with an atom economy of 87% when employing a catalyzed H_2O_2 oxidation process. A further benefit of using enzymatic H_2O_2/alkene epoxidation systems is the ability to work at mild aqueous conditions compared to the elevated temperatures needed to activate H_2O_2 with transition metal salts. The tandem system we report generates H_2O_2 *in situ* and therefore removes the need to store concentrated H_2O_2 solutions which contain stabilisers and will lead to significantly increased reaction volumes due to dilution to appropriate levels for enzyme tolerance. The direct synthesis of H_2O_2 from H_2 and air can potentially achieve 100% atom economy when compared to the anthraquinone process which requires sequential oxidation and reduction of large anthraquinone molecules followed by energy intensive extraction from the organic to aqueous phase. By comparison, the previously reported enzyme cascades used for H_2O_2 delivery utilize either glucose/GOX or sulfites/SO to generate H_2O_2 *in situ*.[17,19,25] The use of a co-substrate in a coupled redox process results in the production of significantly more byproducts (D-gluconic acid or sulfates respectively) by weight than H_2O_2 and consequently a much less atom efficient process for oxidation reactions.

Conclusion

We have demonstrated the combination of a biocatalyst with various chemocatalysts into a tandem catalytic process for oxidation of alkenes to alcohols. In contrast to current industrial technologies, the tandem process is able to operate in aqueous solutions, under mild reaction conditions while producing water as the byproduct. A heterogeneous catalyst produces H_2O_2 *in situ* from abundantly available and cheap resources at levels appropriate for biocatalytic hydroxylation demonstrating an advance in green chemistry and a route to process intensification removing the need to produce and store concentrated H_2O_2 solutions. When alkenes are used as substrates in this process, two competing reaction pathways arise. The first is due to the production of H_2O_2 and subsequent enzymatic oxidation to produce an epoxide (which can subsequently be hydrogenated to a primary alcohol under the same conditions); the second is due to initial hydrogenation of the alkene to an alkane, followed by C–H activation to produce a secondary alcohol. The obtained selectivity of this process may be modulated (to an extent) by careful selection of heterogeneous catalyst to control the relative H_2O_2 synthesis and alkene hydrogenation rates. This result is very promising for future studies on this system combined with further catalyst development to allow production of high yields of either primary or secondary alcohols from terminal alkene substrates in a more facile process with high efficiency.

Experimental

Unspecific peroxygenase preparation

Evolved AaeUPO (PaDa-I variant) designed in *Saccharomyces cerevisiae* was over produced in *Pichia pastoris* in a bioreactor and purified to homogeneity (Reinheitszahl value [Rz] [A_{418}/A_{280}] ~ 2.4) according to previous reports.[22] Enzyme activities was determined in triplicate using ABTS as substrate. 20 μl PaDa-I was added to 180 μl ABTS reaction mixture (100 mM sodium citrate–phosphate pH 4.4 with 0.3 mM ABTS and 2 mM H_2O_2) and substrate conversion was followed by measuring the absorption at 418 nm (ε_{418} = 36 000 M^{-1} cm^{-1}). The PaDa-I concentration was appropriately diluted to give rise to linear enzyme kinetics. One unit is defined as the amount of enzyme that convert 1 μmol of substrate in 1 min.

Catalyst preparation

Mono- and bi-metallic 1 wt%Au_xPd_y/TiO_2 catalysts were prepared by a wet co-impregnation procedure which has been previously reported.[33] To produce 0.5 wt%Au–0.5 wt%Pd/TiO_2 (2 g): Aqueous acidified $PdCl_2$ solution (1.667 mL, 0.58 M HCl, 6 mg mL^{-1}, Sigma Aldrich) and aqueous $HAuCl_4{\cdot}3H_2O$ solution (0.826 mL, 12.25 mg mL^{-1}, Strem Chemicals) were mixed

at 1000 rpm with H_2O (HPLC grade) to a fixed working volume of 16 mL in a 50 mL round bottom flask and thereafter heated to 60 °C. Upon reaching 65 °C, TiO_2 (1.98 g, Degussa, P25 (TiO_2) was added to the continuously agitated solution over the course of 5 minutes. The resulting slurry was stirred at 60 °C for a further 15 min. Following this the temperature was raised to 95 °C for 16 h to allow for complete evaporation of the water. The resulting solid was ground prior to heat treatment in a 5% H_2/Ar atmosphere for 4 h with a ramp rate of 10 °C min^{-1} to 400 °C.

Direct synthesis of H_2O_2

Reactions were carried out in 50 mL gas tight round bottomed flasks rated to 4 bar and stirred using a Radleys 6 Plus Carousel equipped with a gas distribution system. Heterogeneous catalyst powder (2 mg) was weighed directly into the glass flasks. To this was added 10 mL of 100 mM potassium phosphate buffer (pH 6.0) prepared with NaH_2PO_4 and Na_2HPO_4 obtained from Sigma Aldrich. Subsequently, the flask was sealed and pressurized to 2.0 barg with H_2 (1.6 bar) and air (0.4 bar) to give a reaction atmosphere containing 80% H_2 and 20% air. The reaction mixtures were stirred (200 rpm) at 25 °C for 0.5 h, unless otherwise stated. After the desired reaction time the vessel was depressurized and the H_2O_2 concentration determined by UV/Vis spectroscopy. To determine H_2O_2 concentration an aliquot (1.5 mL) of the post reaction solution was combined with potassium titanium oxalate dihydrate solution acidified with 30% H_2SO_4 (0.02 M, 1.5 mL) resulting in the formation of an orange pertitanic acid complex. This resulting solution was analysed spectrophotometrically using an Agilent Cary 60 UV/Vis Spectrophotometer at 400 nm by comparison to a calibration curve by taking aliquots of H_2O_2 in the buffer solution (1.5 mL) and adding acidified potassium titanium oxalate dihydrate solution (1.5 mL). Reaction conditions used within this study to evaluate catalytic performance towards H_2O_2 production operate outside of the flammability limits of gaseous mixtures of H_2 and O_2.

Catalytic testing of the tandem chemo-bio system for hydrocarbon oxidation

Hydrocarbon oxidation reactions were performed in 50 mL gas tight round-bottomed flasks and stirred using a Radleys 6 Plus Carousel equipped with a gas distribution system. Heterogeneous catalyst powder (2 mg unless stated otherwise) was weighed directly into the glass flask. To this was added 10 mL of 100 mM potassium phosphate buffer (pH 6.0) followed by the substrate (20 mM). PaDa-I enzyme was then added at a concentration of 15 U mL^{-1}. Subsequently, the flask was sealed and sequentially pressurized to 2.0 bar with H_2 (1.6 bar) and then with air (0.4 bar). The reaction mixtures were stirred at 200 rpm at 25 °C for 1 h. After 1 h the reaction vessel was placed in an ice bath for 2 minutes and the pressure slowly released. Organic products were extracted using (2 × 5 mL) of ethyl acetate containing 1-decanol (2 mM) as internal standard. A sample was then withdrawn for GC analysis. Components were identified by comparison of retention times with pure reference standards authentic samples. Reaction products obtained during the tandem oxidation of α-methylstyrene were identified by a combination of GC-MS (Fig. S3†) and comparison with reference standards by GC-FID if available. Results reported are the average of at least two duplicate experiments. Product selectivity (%) is defined as mol product per mol total products × 100.

Enzyme deactivation studies

Residual peroxygenase activity was determined by using the substrate 5-nitro-1,3-benzodioxide (NBD) as previously reported.[22]

Catalyst characterization

X-ray photoelectron spectroscopy (XPS) analyses were made on a Kratos Axis Ultra DLD spectrometer. Samples were mounted using double-sided adhesive tape and binding energies were referenced to the C(1s) binding energy of adventitious carbon contamination that was taken to be 284.8 eV. Monochromatic AlK_α radiation was used for all measurements; an analyser pass energy of 160 eV was used for survey scans, while 40 eV was employed for more detailed regional scans. The intensities of the Au(4f) and Pd(3d) features were used to derive the Au/Pd surface composition ratios.

Transmission electron microscopy (TEM) was performed on a JEOL JEM-2100 operating at 200 kV. Samples were prepared by dispersion in ethanol by sonication and deposited on 300 mesh copper grids coated with holey carbon film.

Author contributions

Tandem chemo-bio reactions were carried out by D.W. and S.J.F. under supervision of A.K. and S.T.L.H. Heterogeneous H_2O_2 synthesis studies were carried out by J.B. and R.J.L. Enzyme production in *Pichia pastoris* was carried out by M.A. Enzyme purification was carried out by J.vM. under the supervision of D.J.O. and M.S.S. Transmission electron microscopy was acquired and analyzed by T.E.D. and X-ray photoelectron spectroscopy by D.J.M. The research was directed by S.T.L.H., A.K., M.S.S., G.J.H. and S.J.F. The manuscript was written by D.W., S.J.F. and R.J.L. with input from all authors.

Funding sources

SJF acknowledges the award of a Prize Research Fellowship from the University of Bath and a RSC Research Mobility Grant (RM1802-7768). Financial support from the University of Cape Town and Department of Science and Technology/National Research Foundation Centre of Excellence in Catalysis (C*Change) is also gratefully acknowledged (DW). Further funding and support through the DST-NRF SARChI chair in Bioprocess Engineering (UID 64788), held by STLH, is gratefully acknowledged.

Conflicts of interest

There are no conflicts to declare.

References

1 Y. Ishii, S. Sakaguchi and T. Iwahama, *Adv. Synth. Catal.*, 2001, **343**, 393–427.
2 B. S. Lane and K. Burgess, *Chem. Rev.*, 2003, **103**, 2457–2473.
3 E. M. McGarrigle and D. G. Gilheany, *Chem. Rev.*, 2005, **105**, 1563–1602.
4 G. Shul'pin, *Catalysts*, 2016, **6**, 50–90.
5 A. Jimtaisong and R. L. Luck, *Inorg. Chem.*, 2006, **45**, 10391–10402.
6 M. Mitra, H. Nimir, D. A. Hrovat, A. A. Shteinman, M. G. Richmond, M. Costas and E. Nordlander, *J. Mol. Catal. A: Chem.*, 2017, **426**, 350–356.
7 K. A. Jorgensen, *Chem. Rev.*, 1989, **89**, 431–458.
8 T. Sakaki, *Biol. Pharm. Bull.*, 2012, **35**, 844–849.
9 P. Durairaj, J. S. Hur and H. Yun, *Microb. Cell Fact.*, 2016, **15**, 125.
10 M. Sono, M. P. Roach, E. D. Coulter and J. H. Dawson, *Chem. Rev.*, 1996, **96**, 2841–2888.
11 H. Lin, J. Y. Liu, H. B. Wang, A. A. Q. Ahmed and Z. L. Wu, *J. Mol. Catal. B: Enzym.*, 2011, **72**, 77–89.
12 J. B. Y. H. Behrendorff, W. Huang and E. M. J. Gillam, *Biochem. J.*, 2015, **467**, 1–15.
13 M. Hofrichter and R. Ullrich, *Curr. Opin. Chem. Biol.*, 2014, **19**, 116–125.
14 M. Faiza, S. Huang, D. Lan and Y. Wang, *BMC Evol. Biol.*, 2019, **19**, 76.
15 M. M. C. H. Van Schie, W. Zhang, F. Tieves, D. S. Choi, C. B. Park, B. O. Burek, J. Z. Bloh, I. W. C. E. Arends, C. E. Paul, M. Alcalde and F. Hollmann, *ACS Catal.*, 2019, **9**, 7409–7417.
16 P. Molina-Espeja, S. Ma, D. M. Mate, R. Ludwig and M. Alcalde, *Enzyme Microb. Technol.*, 2015, **73–74**, 29–33.
17 F. Van De Velde, N. D. Lourenço, M. Bakker, F. Van Rantwijk and R. A. Sheldon, *Biotechnol. Bioeng.*, 2000, **69**, 286–291.
18 R. Narayanan, G. Zhu and P. Wang, *J. Biotechnol.*, 2007, **128**, 86–92.
19 F. Tieves, S. J. P. Willot, M. M. C. H. van Schie, M. C. R. Rauch, S. H. H. Younes, W. Zhang, J. J. Dong, P. Gomez de Santos, J. M. Robbins, B. Bommarius, M. Alcalde, A. S. Bommarius and F. Hollmann, *Angew. Chem., Int. Ed.*, 2019, **58**, 7873–7877.
20 M. M. C. H. van Schie, A. T. Kaczmarek, F. Tieves, P. Gomez de Santos, C. E. Paul, I. W. C. E. Arends, M. Alcalde, G. Schwarz and F. Hollmann, *ChemCatChem*, 2020, **12**, 3186–3189.
21 P. Gomez de Santos, S. Lazaro, J. Viña-Gonzalez, M. D. Hoang, I. Sánchez-Moreno, A. Glieder, F. Hollmann and M. Alcalde, *ACS Catal.*, 2020, 13524–13534.
22 S. J. Freakley, S. Kochius, J. van Marwijk, C. Fenner, R. J. Lewis, K. Baldenius, S. S. Marais, D. J. Opperman, S. T. L. Harrison, M. Alcalde, M. S. Smit and G. J. Hutchings, *Nat. Commun.*, 2019, **10**, 4178.
23 W. Zhang, B. O. Burek, E. Fernández-Fueyo, M. Alcalde, J. Z. Bloh and F. Hollmann, *Angew. Chem., Int. Ed.*, 2017, **56**, 15451–15455.
24 W. Zhang, E. Fernández-Fueyo, Y. Ni, M. Van Schie, J. Gacs, R. Renirie, R. Wever, F. G. Mutti, D. Rother, M. Alcalde and F. Hollmann, *Nat. Catal.*, 2018, **1**, 55–62.
25 M. M. C. H. Van Schie, W. Zhang, F. Tieves, D. S. Choi, C. B. Park, B. O. Burek, J. Z. Bloh, I. W. C. E. Arends, C. E. Paul, M. Alcalde and F. Hollmann, *ACS Catal.*, 2019, **9**, 7409–7417.
26 B. O. Burek, S. R. de Boer, F. Tieves, W. Zhang, M. van Schie, S. Bormann, M. Alcalde, D. Holtmann, F. Hollmann, D. W. Bahnemann and J. Z. Bloh, *ChemCatChem*, 2019, **11**, 3093–3100.
27 J. K. Edwards and G. J. Hutchings, *Angew. Chem., Int. Ed.*, 2008, **47**, 9192–9198.
28 J. Sebastian, K. M. Jinka and R. V. Jasra, *J. Catal.*, 2006, **244**, 208–218.
29 G. Xu, Q. H. Xia, X. H. Lu, Q. Zhang and H. J. Zhan, *J. Mol. Catal. A: Chem.*, 2007, **266**, 180–187.
30 M. S. Batra, R. Dwivedi and R. Prasad, *ChemistrySelect*, 2019, **4**, 11636–11673.
31 D. Hua and P. Xu, *Biotechnol. Adv.*, 2011, **29**, 654–660.
32 A. Santos, R. J. Lewis, G. Malta, A. G. R. Howe, D. J. Morgan, E. Hampton, P. Gaskin and G. J. Hutchings, *Ind. Eng. Chem. Res.*, 2019, **58**, 12623–12631.
33 M. Sankar, Q. He, M. Morad, J. Pritchard, S. J. Freakley, J. K. Edwards, S. H. Taylor, D. J. Morgan, A. F. Carley, D. W. Knight, C. J. Kiely and G. J. Hutchings, *ACS Nano*, 2012, **6**, 6600–6613.
34 L. Ouyang, P. F. Tian, G. J. Da, X. C. Xu, C. Ao, T. Y. Chen, R. Si, J. Xu and Y. F. Han, *J. Catal.*, 2015, **321**, 70–80.
35 X. Gong, R. J. Lewis, S. Zhou, D. J. Morgan, T. E. Davies, X. Liu, C. J. Kiely, B. Zong and G. J. Hutchings, *Catal. Sci. Technol.*, 2020, **10**, 4635–4644.
36 R. Imbihl and J. E. Demuth, *Surf. Sci.*, 1986, **173**, 395–410.
37 X. Guo, A. Hoffman and J. T. Yates, *J. Chem. Phys.*, 1989, **90**, 5787–5792.
38 M. Salmeron, *Top. Catal.*, 2005, **36**, 55–63.
39 P. Molina-Espeja, E. Garcia-Ruiz, D. Gonzalez-Perez, R. Ullrich, M. Hofrichter and M. Alcalde, *Appl. Environ. Microbiol.*, 2014, **80**, 3496–3507.
40 M. Piccinini, J. K. Edwards, J. A. Moulijn and G. J. Hutchings, *Catal. Sci. Technol.*, 2012, **2**, 1908–1913.
41 D. I. Enache, J. K. Edwards, P. Landon, B. Solsona-espriu, A. F. Carley, A. A. Herzing, M. Watanabe, C. J. Kiely, D. W. Knight and G. J. Hutchings, *Science*, 2006, **311**, 362–366.
42 H. Lindlar, *Helv. Chim. Acta*, 1952, **35**, 446–450.
43 A. O. King and I. Shinkai, in *Encyclopedia of Reagents for Organic Synthesis*, John Wiley & Sons, Ltd, Chichester, UK, 2001, p. 17.
44 D. Compagnone, A. S. Lupu, A. Ciucu, V. Magearu, C. Cremisini and G. Palleschi, *Anal. Lett.*, 2001, **34**, 17–27.
45 P. N. Nomngongo, J. C. Ngila, V. O. Nyamori, E. A. Songa and E. I. Iwuoha, *Anal. Lett.*, 2011, **44**, 2031–2046.

46 M. E. Ghica, R. C. Carvalho, A. Amine and C. M. A. Brett, *Sens. Actuators, B*, 2013, **178**, 270–278.
47 N. M. Giles, A. B. Watts, G. I. Giles, F. H. Fry, J. A. Littlechild and C. Jacob, *Chem. Biol.*, 2003, **10**, 677–693.
48 D. M. Mate, M. A. Palomino, P. Molina-Espeja, J. Martin-Diaz and M. Alcalde, *Protein Eng., Des. Sel.*, 2017, **30**, 191–198.
49 A. Sasu, B. Dragoi, A. Ungureanu, S. Royer, E. Dumitriu and V. Hulea, *Catal. Sci. Technol.*, 2016, **6**, 468–478.
50 M. M. Telkar, C. V. Rode, R. V. Chaudhari, S. S. Joshi and A. M. Nalawade, *Appl. Catal., A*, 2004, **273**, 11–19.
51 I. Kirm, F. Medina, X. Rodríguez, Y. Cesteros, P. Salagre and J. E. Sueiras, *J. Mol. Catal. A: Chem.*, 2005, **239**, 215–221.
52 B. Notari, *Stud. Surf. Sci. Catal.*, 1988, **37**, 413–425.
53 R. A. Sheldon, *Chem. Soc. Rev.*, 2012, **41**, 1437–1451.